STABILITY OF UNIFORMLY REINFORCED SLOPES

By Radoslaw L. Michalowski,[1] Member, ASCE

ABSTRACT: A limit analysis approach is applied to determine the amount of reinforcement necessary to prevent collapse of slopes due to reinforcement rupture, pullout, or direct sliding. The reinforcement is uniformly distributed over the height of the slope, and each layer of the primary reinforcement has the same length. A rigorous lower bound to the required reinforcement strength is calculated. This formulation is equivalent to that where a strict upper bound to the slope failure height is sought. The length of reinforcement is also calculated; both reinforcement pullout and direct sliding are accounted for. Design charts are produced for both the required reinforcement strength and its length. Although the emphasis is on the analytical considerations, the way results can be practically utilized is shown.

INTRODUCTION

Several methods for the stability analysis of reinforced slopes have been proposed in the last decade, and three different approaches can be distinguished. The first approach is an extension of the conventional "method of slices," in which the reinforcement forces are included in the analysis [see, e.g., Wright and Duncan (1991)]. The second approach (structural) includes considerations of limit equilibrium of multiblock translational mechanisms or a rotational mechanism (Schmertmann et al. 1987; Leshchinsky and Boedecker 1989; Jewell 1990). A continuum approach is the third method used in the stability analysis of reinforced slopes (Sawicki and Leśniewska 1989; de Buhan et al. 1989). The third method is very different from the former two in that the soil and the reinforcement are first homogenized, and the stability analysis involves an anisotropic continuum, rather than two separate constituents (soil and reinforcement).

Both structural and continuum techniques were considered earlier (Michalowski and Zhao 1995) for stability analysis of reinforced soil structures, and the structural approach was found to be more convenient. Calculations in the structural approach can be made using either limit analysis or the limit equilibrium technique. The limit analysis is chosen here (Drucker et al. 1952) since some of the details, such as those related to kinematical admissibility or the influence of soil dilatancy, can be argued more clearly in the context of limit analysis.

A limit analysis solution to the total amount of uniformly distributed reinforcement in slopes (amount necessary to prevent collapse) is presented here. The approach is further extended to estimate the length of the reinforcement. Also, a technique suggested recently for including the effect of pore-water pressure in limit analysis (Michalowski 1995) is applied here. This paper focuses on the stability analysis of reinforced slopes using the kinematic theorem of limit analysis, and it does not address issues related to technology of construction, construction details (for instance, secondary reinforcement), durability, or the level of safety factors that should be used in design.

Stability analysis of reinforced soil slopes has been the subject of several papers leading to design recommendations (Schmertmann et al. 1987; Leshchinsky and Boedecker 1989; Jewell 1990). A set of comprehensive design charts for reinforced slopes was presented by Jewell (1990), and the results in this paper are compared to those later. The differences between the two stem from the different assumptions in the distribution of the reinforcement. Slopes with a uniform distribution of reinforcement strength are considered in this paper, whereas those used often in design presume a triangular distribution.

The technique used here is described briefly in the next section, followed by the formulation of the problem, and the solution. Next, design charts are produced, and the paper ends with some final remarks.

TECHNIQUE USED

The kinematic approach of limit analysis is used here for stability analysis of reinforced slopes. This technique leads to upper bounds to failure loads or critical heights, or the problem can be alternatively formulated to yield the lower bound to the required strength of reinforcement (the latter option is exercised here).

The technique is based on the kinematic theorem of limit analysis. Applicability of this theorem requires that the materials (soil and reinforcement) be perfectly plastic and the deformation be governed by the normality rule. The theorem states that "the rate of work done by traction and body forces is less than or equal to the energy dissipation rate in any kinematically admissible failure mechanism"

$$\int_V \sigma_{ij}^* \dot{\varepsilon}_{ij}^* \, dV \geq \int_S T_i v_i \, dS + \int_V X_i v_i^* \, dV - \int_V u \dot{\varepsilon}_{ii}^* \, dV, \quad i,j = 1, 2, 3 \tag{1}$$

where $\dot{\varepsilon}_{ij}^*$ = strain rate in a kinematically admissible velocity field; $\boldsymbol{\sigma}_{ij}^*$ = stress tensor associated with $\dot{\varepsilon}_{ij}^*$, velocity $v_i^* = v_i$ on boundary S (given boundary condition); $\boldsymbol{X}_i$ = vector of body forces (e.g., specific weight); and S and V = loaded boundary and volume, respectively. The last term in (1) represents the work of the pore-water pressure on the skeleton expansion. Compression is taken here as positive, and the minus sign indicates that positive (compressive) pore pressure u does positive work on the skeleton expansion (negative strain rate). Pore pressure is considered here as an external force, and the failure process is considered to be drained [for details see Michalowski (1995)]. The application of the inequality in (1) for calculating lower bounds to the amount of reinforcement required to avoid a slope collapse is shown in the following sections.

PROBLEM DESCRIPTION

The reinforced slopes considered here are built over foundation soils with the same properties as the slope fill, and mechanisms with failure surfaces extending into the foundation are permitted. The strength of soil is described here by the standard Mohr-Coulomb failure criterion with no cohesion,

[1]Assoc. Prof., Dept. of Civ. Engrg., The Johns Hopkins Univ., Baltimore, MD 21218.

Note. Discussion open until November 1, 1997. To extend the closing date one month, a written request must be filed with the ASCE Manager of Journals. The manuscript for this paper was submitted for review and possible publication on June 12, 1995. This paper is part of the ***Journal of Geotechnical and Geoenvironmental Engineering***, Vol. 123, No. 6, June, 1997. ©ASCE, ISSN 1090-0241/97/0006-0546–0556/$4.00 + $.50 per page. Paper No. 10907.

and the deformation is governed by the normality rule. Reinforcement yielding force of a single layer is characterized by its tensile strength per unit width T_t. The influence of confining stress on the strength of the reinforcement is neglected. The reinforcement layers are distributed uniformly throughout the height of the slope (uniform spacing), and each layer has the same tensile strength. The reinforcement in a slope is characterized here by an average tensile strength k_t defined as

$$k_t = \frac{nT_t}{H} \tag{2}$$

where n = number of reinforcement layers; and H = slope height. For strips of reinforcement, T_t should be taken as the strength of a single strip times the number of strips per unit width of the structure (need not be an integer).

It is convenient to represent the required strength in a dimensionless manner as $k_t/\gamma H$ where γ is the unit weight of the soil. The lower bound solution to required reinforcement strength $k_t/\gamma H$ will be found using the inequality in (1) for slopes of given inclinations and soils with different internal friction angles. This approach is equivalent to seeking an upper bound to the (dimensionless) critical height of slopes $\gamma H/k_t$ (reciprocal of the required reinforcement strength).

The required length of reinforcement also will be calculated from (1), using two different patterns of possible failure. The solution to the reinforcement length presented here is a reasonable estimate, but it is not a rigorous lower bound, since the normal stress on reinforcement is approximated in calculations of the pullout force ($\gamma \times$ depth).

SOLUTION

Limit state analyses (whether kinematic approach or limit equilibrium) are based on considering mechanisms in which the material reaches the limit state and the collapse is imminent. Such mechanisms are then kinematically admissible only when the forces in the reinforcement layers reach their limit (equal to tensile strength or the pullout force). Therefore, we will refer here to the reinforcement force distribution as the distribution of reinforcement strength.

It was found earlier (Chen 1975) that the rotational collapse mechanism leads to the least upper bounds to critical heights of unreinforced slopes with traction-free boundaries. The analysis that follows involves a log-spiral failure surface consistent with the rotational mechanism. In calculations of the required reinforcement length, however, both the rotational and translational mechanisms are considered.

Required Strength of Reinforcement

The failure surface is described by the log-spiral equation

$$r = r_0 e^{(\theta-\theta_0)\tan\varphi} \tag{3}$$

where φ = internal friction angle of the soil; and r_0 = radius of the log-spiral related to angle θ_0 (Fig. 1). The admissibility of the rotational failure requires that the velocity jump vector be inclined at angle φ to the failure surface, and its magnitude propagates according to

$$v = \dot{\omega} r_0 e^{(\theta-\theta_0)\tan\varphi} \tag{4}$$

where $\dot{\omega}$ = rate of rotation of the moving mass.

With the normality rule and zero cohesion, the stress vector on the failure surface and the velocity jump vector are mutually perpendicular; hence the energy dissipation rate in the soil along the failure surface during collapse is zero. The only contribution to dissipation on the left-hand side of (1) is that from the reinforcement. For a traction-free slope the nonzero terms on the right-hand side of (1) are those due to the soil weight and pore-water pressure.

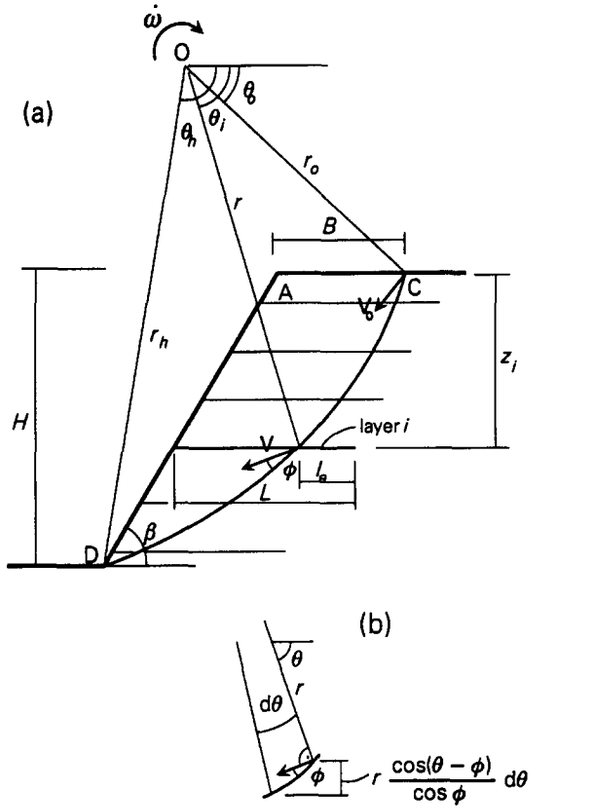

FIG. 1. Rotational Failure Mechanism: (a) Log-Spiral Failure Surface; (b) Infinitesimal Increment

The dissipation rate in the reinforcement per infinitesimal increment of the failure surface is equal to the dot product of the force in the reinforcement and the velocity jump vector $\mathbf{v}$ [Fig. 1(b)]

$$d\dot{D} = k_t r\, d\theta \frac{\cos(\theta - \varphi)}{\cos\varphi} \mathbf{n}\cdot\mathbf{v} \tag{5}$$

where $\mathbf{n}$ = a unit vector in the direction of the reinforcement. From (3) and (4), the increment of the dissipation rate in (5) can be written as

$$d\dot{D} = k_t \dot{\omega} r_0^2 (\sin\theta\cos\theta + \sin^2\theta\tan\varphi) e^{2(\theta-\theta_0)\tan\varphi}\, d\theta \tag{6}$$

The expression in (6) is now integrated in the range from θ_0 to θ_h [Fig. 1(a)] to yield

$$\dot{D} = \frac{1}{2} k_t \dot{\omega} r_0^2 [\sin^2\theta_h e^{2(\theta_h-\theta_0)\tan\varphi} - \sin^2\theta_0] \tag{7}$$

An identical energy dissipation rate results from an analysis with a discrete distribution (with uniform spacing) of reinforcement.

With no traction on the surface of the slope, the expression on the right-hand side of (1) reduces to two terms describing the work rate of the soil weight, $\dot{W}_\gamma$, and the contribution of the pore-water pressure. The first term can be derived in a closed form by calculating the rate of work of a fictitious soil mass in region OCDO, and subtracting the rates for regions OCAO and ODAO [Fig. 1(a)]. Consequently, for a toe failure mechanism, the rate of work of the soil weight can be written in the following form:

$$\dot{W}_\gamma = \gamma r_0^3 \dot{\omega}(f_1 - f_2 - f_3) \tag{8}$$

where f_1, f_2, and f_3 = functions of slope inclination angle (β), the geometry of the failure surface (θ_0, θ_h), and the internal friction angle of the soil (φ). These functions were derived

earlier by Chen et al. (1969), and, for completeness, are given in Appendix I.

The influence of the pore water is included in the last term of (1). This term represents the rate of work of the pore-water pressure on the volumetric (dilative) deformation of sand, and can be written as

$$\dot{W}_u = \gamma r_0^3 \dot{\omega} r_u f_5 \tag{9}$$

where r_u = pore pressure coefficient as defined by Bishop and Morgenstern (1960); and f_5 = a function of geometry and φ (given in Appendix I). Equating the energy dissipation rate in (7) to the rate of work in (8) and (9) leads to the expression for the lower bound to the dimensionless required strength of reinforcement

$$\frac{k_t}{\gamma H} = \frac{2(f_1 - f_2 - f_3 + r_u f_5)}{\sin^2\theta_h e^{2(\theta_h - \theta_0)\tan\varphi} - \sin^2\theta_0} \frac{r_0}{H} \tag{10}$$

where r_0/H is derived from geometrical relations in Fig. 1(a)

$$\frac{H}{r_0} = \sin\theta_h e^{(\theta_h - \theta_0)\tan\varphi} - \sin\theta_0 \tag{11}$$

and functions f_i are given in Appendix I [function f_4 is deliberately omitted in (10); it is used only for below-the-toe failures not considered here]. Eq. (10) represents the rigorous lower bound to (dimensionless) uniformly distributed required strength of reinforcement $k_t/\gamma H$ (or it can be rearranged to yield the upper bound to the critical height of slopes $\gamma H/k_t$).

The expression in (10) is valid for admissible combinations of θ_0 and θ_h, and, since it represents the lower bound, an optimization scheme needs to be used to find the maximum of $k_t/\gamma H$, with θ_0 and θ_h being variables. The charts for the required amount of reinforcement based on (10) are produced later (section titled "Design Charts").

When $\theta_h > \pi/2 + \varphi$ the failure surface reaches deep into the slope base (assumed to have the same properties as the fill), and it passes through the unreinforced soil. It can be shown, however, that the expression in (10) is valid for such cases.

It also should be pointed out that when $\theta_0 < 0$, the center of rotation is located below the slope crest, and the reinforcement in the top part of the slope may be in compression (this is illustrated later in this section). This reinforcement contribution to stability is neglected here since it is likely to kink or buckle. For such instances the energy dissipation rate in (6) needs to be integrated from 0 to θ_h. The expression in (7) will then become

$$\dot{D} = \frac{1}{2} k_t \dot{\omega} r_0^2 \sin^2\theta_h e^{2(\theta_h - \theta_0)\tan\varphi} \tag{12}$$

and the required reinforcement strength in expression (10) will change accordingly. It was found from calculations based on (10) that cases where $\theta_0 < 0$ for the critical slip surface occur only for steep slopes with significant pore-water pressure.

Length of Reinforcement

Two qualitatively different failure mechanisms are considered in calculations of the minimum reinforcement length: rotational collapse with some reinforcement layers being pulled out of the soil, and a translational mechanism where the entire reinforced soil mass "slides" over one reinforcement layer. The first collapse pattern is termed here a "pullout" (or overall) failure, and the second one will be referred to as a "direct sliding" mode.

Reinforcement Length—Pullout Mechanism

The length of reinforcement needs to be such that the required strength calculated from (10) does not need to be increased because of the possibility of pullout failure in some layers. In other words, the most adverse failure mechanism involving the combination of the tensile failure in some layers and pullout in others needs to provide a required reinforcement strength, which is no larger than that in (10). An economical design requires, of course, that the reinforcement not be longer than necessary.

Common to most techniques is the assumption that the pullout force of a reinforcement layer per unit of its width, T_p, is proportional to the overburden pressure γz^*, effective length l_e [Fig. 1(a)], and friction coefficient between the soil and reinforcement μ_b

$$T_p = 2\gamma z^*(1 - r_u) l_e \mu_b \tag{13}$$

The overburden depth z^* for gentle slopes may be less than depth z of the reinforcement below the slope crest. For strip reinforcement, (13) has to be multiplied by the ratio of a single strip width over the unit width times the number of strips per unit width (need not be an integer). Coefficient μ_b (Jewell 1990) is expressed as a fraction of the tangent of the soil internal friction angle

$$\mu_b = f_b \tan\varphi \tag{14}$$

where f_b = a "bond coefficient." In what follows, the required reinforcement strength is derived considering that some reinforcement layers fail in the pullout mode ($T_p < T_t$).

The effective length l_{ei} of reinforcement layer i can be derived from geometrical relations in Fig. 1(a) as

$$l_{ei} = L + (\cos\theta_h + \sin\theta_h \cot\beta) r_0 e^{(\theta_h - \theta_0)\tan\varphi} - (\cos\theta_i + \sin\theta_i \cot\beta) r_0 e^{(\theta_i - \theta_0)\tan\varphi} \tag{15}$$

where L = reinforcement length; and θ_i = angle related to reinforcement layer i [Fig. 1(a)]. The following relation holds:

$$\sin\theta_i e^{(\theta_i - \theta_0)\tan\varphi} = \sin\theta_0 + \frac{z_i}{r_0} \tag{16}$$

where z_i = depth of the ith reinforcement layer. Since the distribution of the reinforcement strength is assumed to be uniform, the following expression is used to calculate the depth of the reinforcement layers:

$$z_i = (i - 0.5)\frac{H}{n}, \quad i = 1, 2, \ldots, n \tag{17}$$

The procedure of deriving the required $k_t/\gamma H$ is the same as earlier, but the energy dissipation rate is now calculated separately for reinforcement layers failing in tension ($\dot{D}_t$) and for those being pulled out ($\dot{D}_p$)

$$\dot{D}_p = \sum_{i=1}^{k} T_p r_0 \dot{\omega} \left(\sin\theta_0 + \frac{z_i}{r_0}\right); \quad \dot{D}_t = \sum_{i=k+1}^{n} T_t r_0 \dot{\omega} \left(\sin\theta_0 + \frac{z_i}{r_0}\right) \tag{18a,b}$$

where k = number of layers that are pulled out (for which $T_p < T_t$); and n = total number of reinforcement layers. Considering that force T_t can be expressed as a function of k_t [see (2)], the dimensionless required strength assumes the form

$$\frac{k_t}{\gamma H} = \left\{\left(\frac{r_0}{H}\right)^2 (f_1 - f_2 - f_3 + r_u f_5) - 2 f_b \tan\varphi(1 - r_u) \cdot \sum_{i=1}^{k} \left[\frac{z_i^*}{H}\frac{l_{ei}}{H}\left(\sin\theta_0 + \frac{z_i}{r_0}\right)\right]\right\} \Big/ \frac{1}{n}\sum_{i=k+1}^{n}\left(\sin\theta_0 + \frac{z_i}{r_0}\right) \tag{19}$$

The reinforcement strength in (19) is no longer a strict lower bound, since the pullout force is only approximately calculated in (13). Nevertheless, (19) is a reasonable estimate. Although (19) seems complex, it is conceptually a straightforward result.

It is obtained with the minimum number of assumptions within the framework of limit analysis. For the reinforcement to be used economically, its length should be such that $k_t/\gamma H$ calculated from (19) is the same as that in (10).

The length of the reinforcement L is included in the effective length in the numerator of (19) [see also (15)]. Having calculated $k_t/\gamma H$ from (10), and substituted it for the left-hand side of (19), an implicit equation results for L. This equation needs to be solved iteratively for a given geometry of the failure surface expressed by angles θ_0 and θ_h. This procedure leads to a lower bound on the length of reinforcement, and an optimization procedure was used to find maximum L with θ_0 and θ_h being variable.

It can be noticed that, while for a slope failure with tensile rupture in all reinforcement layers the solution is independent of the number of reinforcing layers n [see (10)], consideration of pullout makes the result dependent on n (the sensitivity to the number of layers may drop down with an increase in n, nT_t being constant).

The concept behind the reinforcement length criterion used here is illustrated in Fig. 2. The length of the reinforcement in the slope shown is $L = 0.535H$ ($\beta = 70°$, $\varphi = 35°$, $r_u = 0$). The bold line in Fig. 2(a) shows the dimensionless required reinforcement strength as a function of coordinate x at which the failure surface intersects the crest of the slope. Point A relates to the most adverse (critical) mechanism in which all reinforcement layers fail in tension.

If the failure surface is "moved" to the right [from A toward B in Fig. 2(b)], the calculated strength of reinforcement needed to maintain limit equilibrium will decrease (the new location of the failure surface is not as critical as that at A). When the failure surface is moved even further toward B, the effective length of the top layer of reinforcement decreases, and this layer starts to pull out rather than rupture. Consequently, $k_t/\gamma H$ varies with the change in the failure surface location because of the two competing effects: a stabilizing effect of the soil weight due to movement of the failure surface further away from its most detrimental position, and an adverse effect due to reduction in effective reinforcement length leading to a drop in the limit force in some reinforcement layers (from their tensile strength to the pullout force).

The lower bound to required reinforcement reaches a maximum at point A (all reinforcement layers fail in tension), reaches a local maximum at point B (with the top layer being pulled out), then reaches a local minimum at point C, and another maximum at D. The failure surface marked as D [Fig. 2(b)] bypasses the two top layers of the reinforcement and the third layer is pulled out. For the reinforcement to be fully utilized, its length needs to be estimated so that the magnitude of the maximum of $k_t/\gamma H$ at point D will be the same as that at A (i.e., that failure surfaces A and D are both critical). For this particular case it is: $L = 0.535H$.

An increase in the length of reinforcement beyond $L = 0.535H$ will not decrease the required reinforcement strength (or, it will not increase the slope safety), since it only reduces the maximum of $k_t/\gamma H$ at D, and the best lower bound to the required reinforcement remains at A. Results of calculations for $L = 0.55H$ are also shown in Fig. 2(a). A reduction in length, however, would cause an increase in required reinforcement, since the maximum at D would now increase; a case for $L = 0.52H$ is also marked in Fig. 2(a).

The geometry of the log-spiral failure surface intersecting the slope toe is described by two parameters. Calculations of results presented in Fig. 2(a) were made using an optimization procedure where only one parameter was varied (θ_0), whereas the second parameter was used to ensure the required coordinate x [Fig. 2(a)].

Some peculiar cases are shown in Figs. 3(a) and 3(b) [these were indicated earlier in Michalowski (1996)]. Each of the figures presents a slope with the two most adverse failure surfaces (A and D), which correspond to maxima of $k_t/\gamma H$ similar to those in Fig. 2(a). Failure surface A in Fig. 3(a) relates to a rotational mechanism with a center of rotation below the slope crest. This was found to be the case for steep slopes with

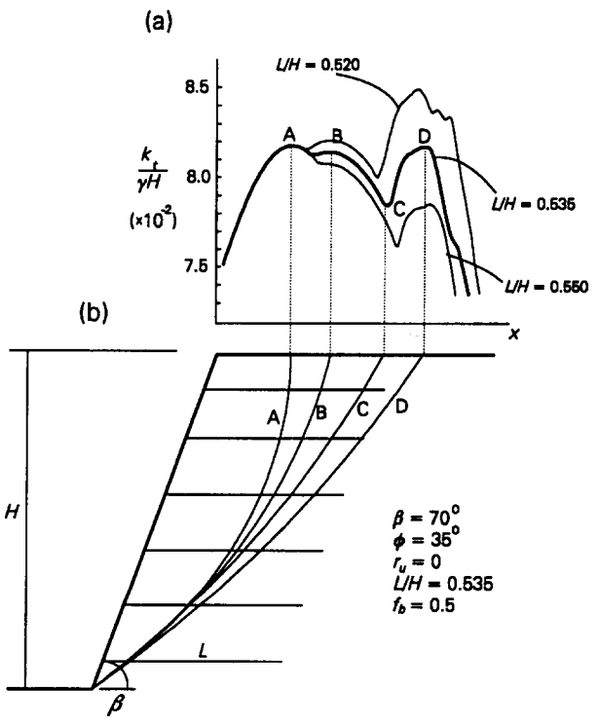

FIG. 2. Criterion for Estimates of Required Length of Reinforcement: (a) Required Strength for Varied Failure Surfaces; (b) Failure Surfaces Correlated to Maxima and Local Minimum of Required Strength for $L/H = 0.535$

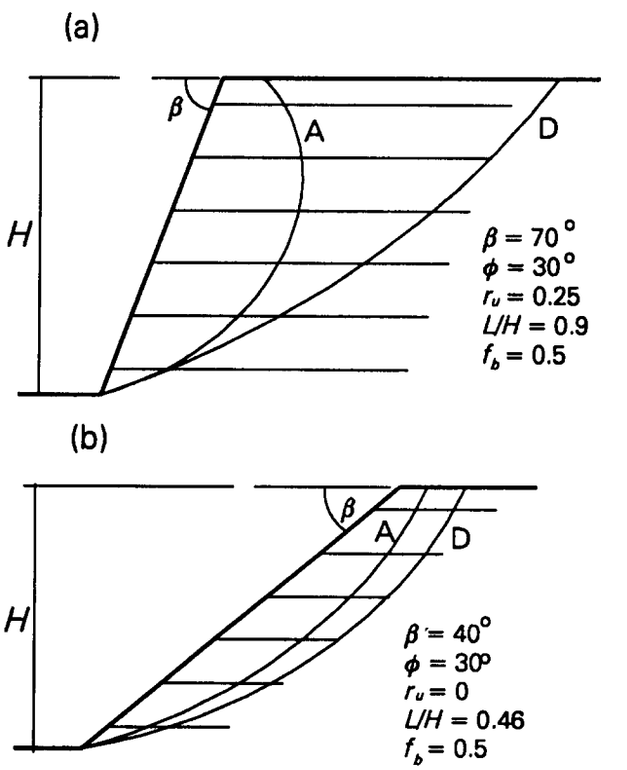

FIG. 3. Reinforced Slopes with Critical Failure Surfaces: (a) Steep Slope; (b) "Shallow" Slope

a significant pore-water pressure. In such an instance the top layer/layers may be subjected to compression; this occurs when $\sin \theta_0 + z_i/r_0 < 0$. A term for layer i should then be omitted (taken as zero) in the summation in (19) (it also should be taken as 0 if the failure surface does not intersect the reinforcement).

In some cases the reinforcement layers that are pulled out during collapse may not necessarily be the top ones, and the summation in (19) may not be in the sequence in which the layers appear in the soil. This is presented in Fig. 3(b) (surface D), where the tensile strength in the top two layers is fully utilized, while the third layer (from the top) contributes very little to stability (small effective length), and the fourth one contributes nothing.

Reinforcement Length—Direct Sliding Mechanism

The direct sliding mechanism is shown in Fig. 4. The rotation of the soil mass is incompatible with the direct sliding (translation) pattern. In the incipient mechanism considered, block BCED moves with velocity v_0, and block ABD moves with velocity v_1. The coefficient of friction in direct sliding μ_d is expressed here as fraction f_d of $\tan \varphi$

$$\mu_d = \tan \varphi_w = f_d \tan \varphi \tag{20}$$

where f_d = a direct sliding coefficient. The normality rule requires that v_0 and $[v]$ be inclined at angle φ to surfaces BC and BD, respectively, and vector $\mathbf{v}_1$ be inclined at φ_w to reinforcement surface AB. The hodograph in Fig. 4(b) is used to calculate magnitudes of $\mathbf{v}_1$ and $[v]$ as functions of $\mathbf{v}_0$. All layers of reinforcement are of equal length L. The geometry of blocks in Fig. 4(a) can be represented as functions of L and the depth to the layer over which sliding occurs. This depth here is assumed to be equal to the slope height H. Rupture surface BC may or may not intersect the reinforcement.

The lower bound to the necessary length is calculated from the theorem in (1). As the slope boundaries are load free, the first term on the right-hand side is equal to zero, and the length of reinforcement is implicitly included in all nonzero terms in (1). The term on the left-hand side includes dissipation during pullout of reinforcement along BD (and along BC if $\alpha > \beta$).

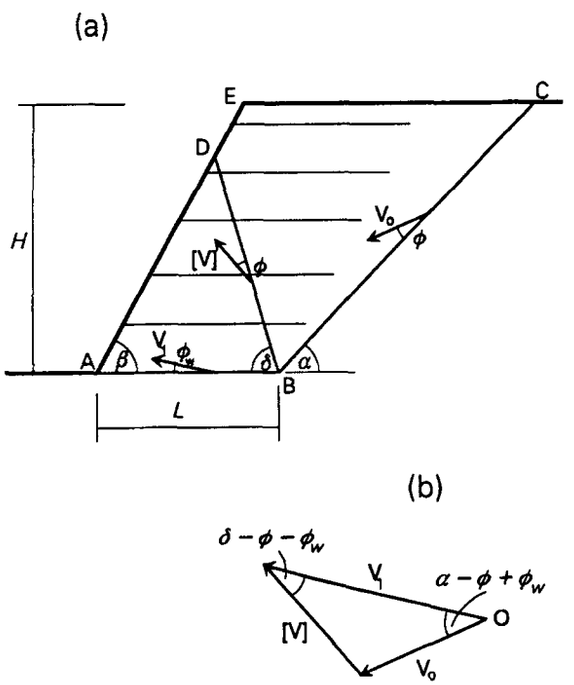

FIG. 4. Direct Sliding: (a) Collapse Mechanism; (b) Hodograph

The results (design charts) produced later include cases for which the required length calculated was the maximum (angles α and δ were variables in an optimization scheme).

Literature on the active pressure problem [for instance, Chen (1975)] indicates that one plane failure surface (BC) is a good approximation of the most adverse translational collapse mechanism. Four different cases were distinguished, depending on the reinforcement length, involvement of the pore-water pressure, and location of point D in relation to point E (Fig. 4). Equations describing the required length of reinforcement to prevent direct sliding are all linear or parabolic. These equations are of an algebraic nature, and the details are omitted here.

DESIGN CHARTS

The expression in (10) was used to calculate the lower bound to the required strength of reinforcement represented by dimensionless parameter $k_r/\gamma H$, as a function of slope inclination angle β and the internal friction angle of the slope fill. The results of calculations are shown in diagrams [Figs. 5(a)–(c)] for pore-water pressure coefficient r_u equal to 0, 0.25, and 0.5, respectively, for slope inclination angles in the range of 30–90°, and the internal friction angle of 20–50°. A reasonable angle of internal friction for slope design does not exceed 40°. The results for larger φ are shown here to make the comparison to other charts (Jewell 1990) more comprehensive. An optimization scheme was used in which angles θ_0 and θ_h were varied (with a minimum step of 0.05°) and the maximum of $k_r/\gamma H$ was sought.

The failure mechanism can extend into the foundation soil, which has the same properties as the slope fill. If the foundation soil is assumed to be rigid (i.e., if condition $\theta_0 \leq \theta_h \leq \pi/2 + \varphi$ is enforced), the calculations are affected only when the pore pressure coefficient is significant. The tendency of the solution for slopes on a rigid foundation is indicated by segments of dashed lines in Figs. 5(b,c). A peculiar solution is obtained for $\varphi = 20°$ and $r_u = 0.5$, where a slope of inclination $\beta = 45°$ requires slightly more reinforcement than that with $\beta = 65°$. This seems to be caused by the pore-water pressure, the adverse influence of which increases with the increase in depth of the failure mechanism.

Calculations of the required length of the reinforcement are more complex. For the reinforcement to be fully utilized the required reinforcement calculated considering either pullout failure [(19)] or direct sliding should be the same as in (10).

Charts for reinforcement length $(L/H)_{ovrl}$, including the most adverse combination of pullout and rupture of reinforcement layers in a rotational failure mode ("overall" failure), are given in Fig. 6. Calculations were performed assuming six layers of reinforcement, and coefficient $f_b = 0.5$ and 0.8. The calculations revealed a rather small difference between the results for different f_b (a few percent). This is understandable in cases where only one or two layers are pulled out. When the most adverse mechanism included rupture of some reinforcement layers while the remaining ones did not intersect the failure surface at all, the result was, of course, independent of coefficient f_b (i.e., an increase in f_b would not produce a decrease in required length). To restrict the number of charts, only the results for $f_b = 0.5$ are presented in Fig. 6. Some "irregularities" were noticed in the results; these were identified as being caused by the discrete distribution of reinforcement (the charts in Fig. 6 were gently smoothened).

Finally, the minimum length of reinforcement required to prevent the direct sliding failure mode $(L/H)_{ds}$ is shown in Fig. 7. The charts are shown for $f_d = 0.8$, which is a reasonable value for most geosynthetics. Coefficient $f_b = 0.5$ was used in calculations of pullout forces along rupture surfaces BD (and BC if $\alpha > \beta$, Fig. 4).

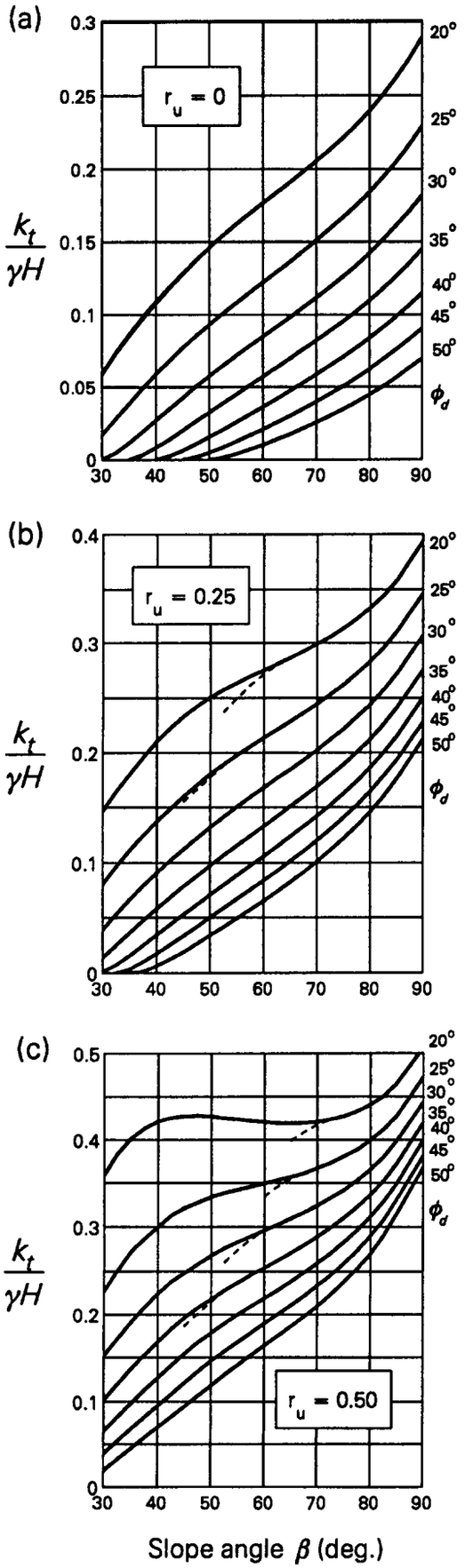

FIG. 5. Required Strength of Uniformly Distributed Reinforcement in Slopes; Design Charts for: (a) $r_u = 0$; (b) $r_u = 0.25$; (c) $r_u = 0.50$

The charts in Figs. 6 and 7 are based on calculations for slopes with six reinforcement layers, and the required length changes (drops) with an increase in the number of layers. The charts in this paper are applicable for slopes with a number of layers not less than six, and should be applied more cautiously for slopes with a smaller number of reinforcement layers.

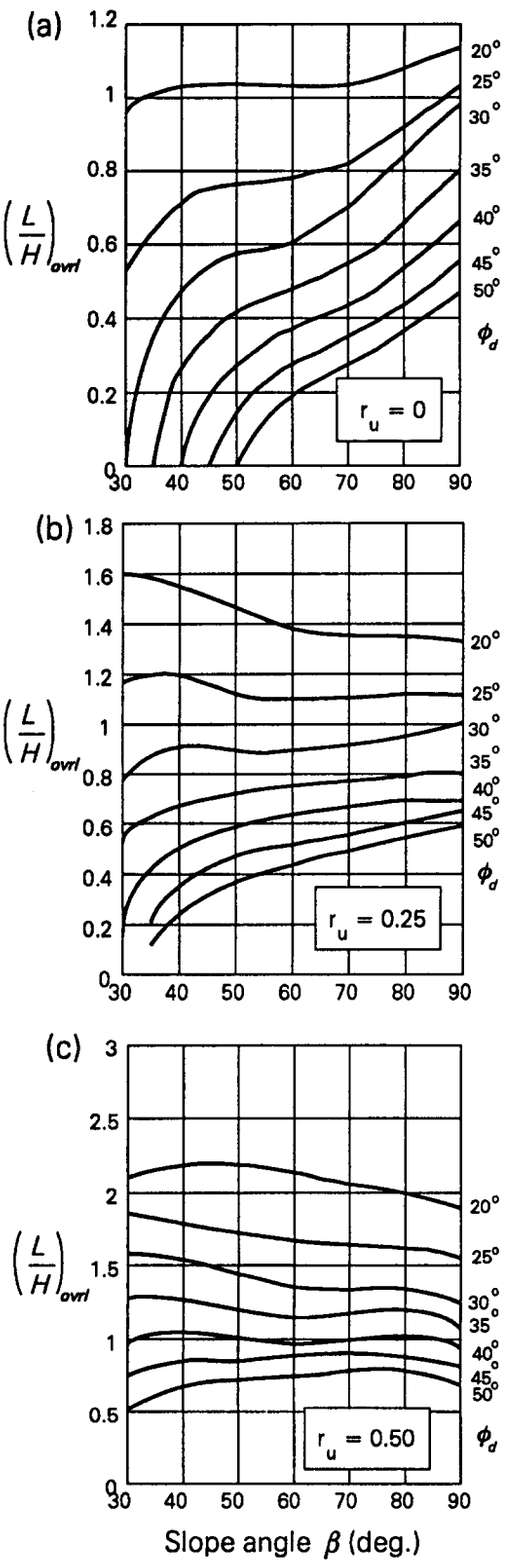

FIG. 6. Reinforcement Length for Slopes, Overall (Pullout and Rupture) Failure; Design Charts for Six Layers with Uniform Spacing: (a) $r_u = 0$; (b) $r_u = 0.25$; (c) $r_u = 0.50$

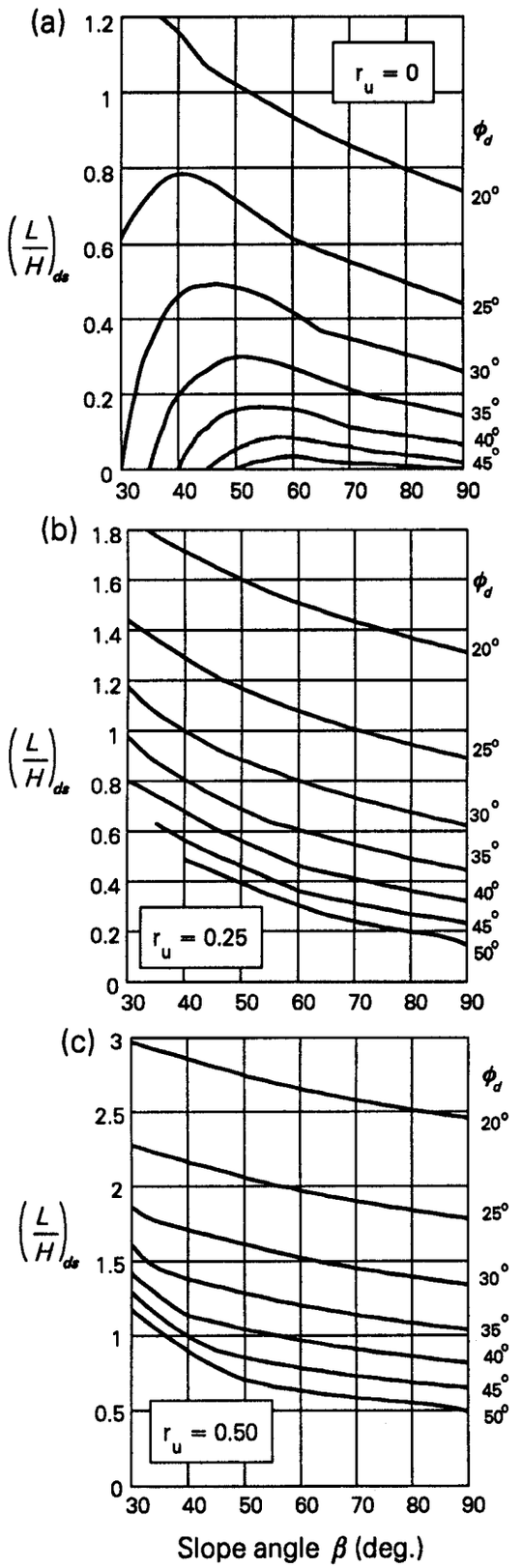

FIG. 7. Reinforcement Length for Slopes, Direct Sliding; Design Charts for Six Layers with Uniform Spacing: (a) $r_u = 0$; (b) $r_u = 0.25$; (c) $r_u = 0.50$

The focus of this paper is on the solution (and the solution technique), and not as much on the design. However, it is indicated very briefly how one can determine the number of layers (or spacing) using the solution charts. Once $k_t/\gamma H$ is determined from the charts (for a slope of given inclination), referring to the definition of k_t in (2), one can find the lower bound to the number of reinforcement layers when the strength of a single layer, T_t, is given

$$n = k_t \frac{H}{T_t} \tag{21}$$

or vice versa. It is not suggested that either the peak or the critical (large strain) value of the internal friction angle should be used in every design. The decision may be influenced by the designer's confidence in the test data and the expected variability of the fill. The use of the critical state friction angle is certainly prudent, but it may be overconservative. In either case, $k_t/\gamma H$ should be read from the diagrams in Fig. 5 for the reduced value φ_d

$$\varphi_d = \tan^{-1}\left(\frac{\tan \varphi}{F}\right) \tag{22}$$

where F = factor of safety. T_t in (21) is the strength of a single layer including the necessary partial safety factors (due to creep, chemical/biological deterioration, construction damage, etc.). The necessary length L can be obtained from Figs. 6 and 7 (larger L should be used in design), and the depth of the layers can be calculated from the formula in (17).

COMPARISON TO OTHER RESULTS

It is useful to compare the results to existing solutions to indicate any differences, sources of these differences, and possible consequences in design. Design charts presented by Jew-

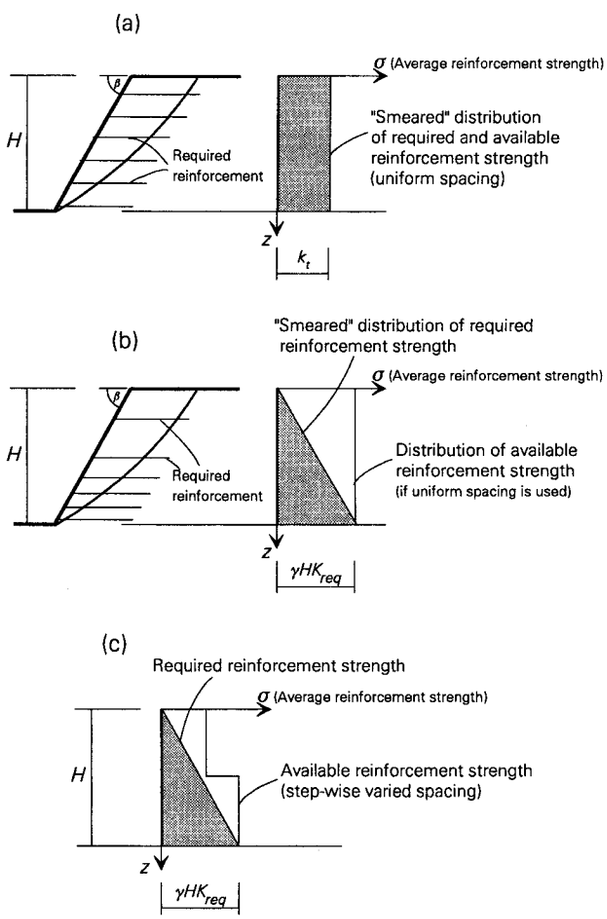

FIG. 8. Required Reinforcement Strength: (a) Uniform Reinforcement; (b) Triangular Distribution; (c) Triangular Distribution and Stepwise Varied Spacing

ell (1990) are selected for comparison as they seem to be the most comprehensive in their scope, and also those by Schmertmann et al. (1987).

Slopes with uniformly distributed reinforcement (evenly spaced reinforcement layers of equal strength) were considered in this paper. If the strength of such reinforcement is distributed continuously ("smeared") through the slope height, it can be represented by the shaded area in Fig. 8(a). Design charts were produced based on the analysis of a rotational failure. Jewell's calculations are based on the same (rotational) mechanism, but with a triangular reinforcement force distribution [the shaded area in Fig. 8(b)]. In the framework of limit analysis the difference between calculations with uniform and triangular distributions of reinforcement strength appears in the work dissipation rate during failure. For triangular distribution the expression in (7) would read

$$\dot{D} = \frac{1}{3} k_t \dot{\omega} r_0^2 [2 \sin^2\theta_h e^{2(\theta_h - \theta_0)\tan\varphi} - \sin\theta_0 \sin\theta_h e^{(\theta_h - \theta_0)\tan\varphi} - \sin^2\theta_0] \tag{23}$$

and the lower bound to the average reinforcement strength becomes

$$\frac{k_t}{\gamma H} = \frac{3(f_1 - f_2 - f_3 + r_u f_5)}{2 \sin^2\theta_h e^{2(\theta_h - \theta_0)\tan\varphi} - \sin\theta_0 \sin\theta_h e^{(\theta_h - \theta_0)\tan\varphi} - \sin^2\theta_0} \frac{r_0}{H} \tag{24}$$

The results in Jewell's (1990) charts are given in terms of required coefficient K_{req}, which can be expressed as a function of k_t

$$K_{req} = 2 \frac{k_t}{\gamma H} \tag{25}$$

TABLE 1. Comparison of Required Reinforcement (K_{req})[a] for Slopes ($r_u = 0$)

Slope angle β (°) (1)	Internal friction angle φ (°) (2)	Uniform reinforcement [Eq. (10)] (3)	Triangular reinforcement [Eq. (24)] and Jewell (1990) (4)	Schmertmann et al. (1987) (5)
40	20	0.218	0.188	0.22
40	30	0.054	0.049	0.05
60	20	0.353	0.285	0.37
60	30	0.169	0.146	0.17
60	40	0.073	0.064	0.07
80	20	0.479	0.394	0.48
80	30	0.285	0.251	0.30
80	40	0.167	0.151	0.18

[a] $K_{req} = 2k_t/\gamma H$.

Calculations of maximum $k_t/\gamma H$ were performed using (24) (with θ_0 and θ_h being variable), and the results are the same as those in Jewell's (1990) charts. Only for large pore-water pressure, $r_u = 0.5$, steep slopes, and large internal friction angles are the charts in Jewell (1990) excessively "smoothened" (for instance, for $\beta = 70°$ and $\varphi = 50°$ the charts read $K_{req} \approx 0.36$, while the calculations based on identical assumptions yield $K_{req} = 0.319$).

A comparison of numerical results obtained in this paper (uniform reinforcement) to those found in Jewell (1990) and Schmertmann et al. (1987) (both with a triangular distribution of the reinforcement limit force) is given in Tables 1–3. Results are shown in Table 1 in terms of K_{req} [(25)] for selected parameters. The numbers in columns 3 and 4 were calculated using (10) and (24), respectively. The numbers in column 5 are taken from Schmertmann et al. (1987). The latter are based on an approximate two-wedge mechanism and were modified by their authors to be consistent with results from the Bishop and Spencer methods. The larger the K_{req}, the larger the strength (or amount) of reinforcement necessary to avoid collapse.

In terms of the total amount of reinforcement, the analysis presented here yields a larger amount than in Jewell (1990), and the results are somewhat closer to those of Schmertmann et al. (1987). These results are not at all surprising. When a rotational mechanism is considered, it is the moment of reinforcement force (with respect to the center of rotation) that is being estimated, and not the reinforcement force itself. The resultant force for a triangular reinforcement distribution is located at one-third of the slope height, and it provides a larger resisting moment than a resultant force of the same magnitude but for a uniformly distributed reinforcement. Consequently, a lesser amount of the reinforcement with a triangular force distribution is required to provide the same resisting moment.

The difference between the results in columns 3 and 4 of Table 1 becomes more significant for slopes with large pore-water pressure.

Design charts based on a triangular distribution of the reinforcement force are often used in a very conservative manner (particularly for "short slopes"), where a uniform spacing of the reinforcement is calculated based on the required strength at the bottom of the slope, $\gamma H K_{req}$ [Fig. 8(b)]. In doing so, the amount of reinforcement is "silently" doubled in addition to any safety factors used. The total required limit force in the reinforcement consistent with the assumption of triangular distribution of reinforcement strength is equal to the integral of the shaded area in Fig. 8(b), whereas the design strength (when uniform spacing is used) is depicted by the solid vertical line. The reinforcement will be less than doubled, however (but still will exceed the necessary amount), if varied spacing is designed [Fig. 8(c)], which is routinely done for high slopes ($H > 6$ m).

TABLE 2. Comparison of Required Reinforcement Length $(L/H)_{req}$ for Slopes ($r_u = 0$)

Slope angle β (°) (1)	Internal friction angle φ (°) (2)	Uniform Reinforcement [Eqs. (19) and (17)] $n = 6$, $f_b = 0.5$ (3)	$n = 6$, $f_b = 0.9$ (4)	$n = 50$, $f_b = 0.9$ (5)	Triangular [Eqs. (19) and (26)] $n = 6$, $f_b = 0.9$ (6)	$n = 50$, $f_b = 0.9$ (7)	Jewell (1990)[a] — (8)	Schmertmann et al. (1987)[b] $f_b = 0.9$ (9)
40	20	1.085	1.065	0.960	1.025	1.000	1.05	0.98
40	30	0.460	0.460	0.435	0.460	0.445	0.47	0.29
60	20	1.005	0.985	0.950	0.885	0.840	0.84	0.89
60	30	0.605	0.600	0.580	0.525	0.505	0.51	0.52
60	40	0.370	0.365	0.355	0.320	0.310	0.31	0.28
80	20	1.080	1.025	0.935	0.935	0.805	0.80	0.80
80	30	0.840	0.725	0.675	0.645	0.565	0.57	0.56
80	40	0.525	0.520	0.485	0.455	0.410	0.40	0.42

[a] Numbers read from diagrams in Jewell (1990).
[b] Length marked as L_T (top) given in Schmertmann et al. (1987).

TABLE 3. Comparison of Required Reinforcement Length $(L/H)_{de}$ for Slopes ($r_u = 0$)

Slope angle β (°) (1)	Internal friction angle φ (°) (2)	Charts in Fig. 7 $f_d = 0.8$ (3)	Jewell (1990) $f_d = 0.8$ (4)	Schmertmann et al. (1987) $f_d = 0.9$ (5)
40	20	1.160	1.27	1.18
40	30	0.459	0.50	0.44
60	20	0.934	0.98	0.98
60	30	0.417	0.45	0.52[a]
60	40	0.161	0.16	0.28[a]
80	20	0.795	0.72	0.80[a]
80	30	0.306	0.30	0.56[a]
80	40	0.090	0.08	0.42[a]

[a]Larger of two numbers (for top and bottom of the slope) given in Schmertmann et al. (1987).

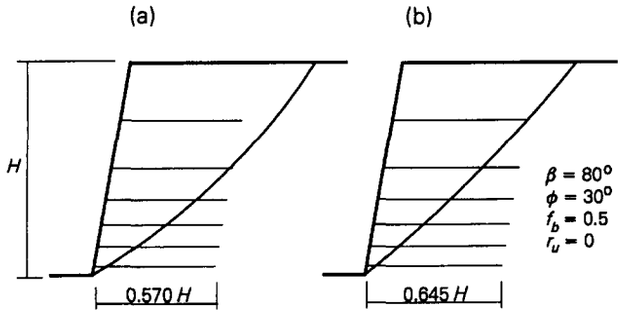

FIG. 9. Failure Surfaces Related to Maxima of Required Reinforcement Length: (a) Local Maximum of 0.57*H*; (b) Global Maximum of 0.645*H*

Comparison of the required reinforcement length is presented in Tables 2 and 3. Required length calculated using the uniform distribution of reinforcement [(19)] is shown in columns 3–5 of Table 2, for a different number of layers, n, and different "bond coefficient" f_b. Results by Jewell (1990) are independent of the number of layers and f_b (column 8), and those by Schmertmann et al. (1987) are independent of n (column 9). The last two are in good agreement, whereas the calculations based on the uniform distribution of reinforcement usually indicate larger length. The differences are understandable, considering different assumptions (reinforcement distribution).

In an attempt to calculate a reinforcement length consistent with the assumptions of triangular distribution of reinforcement strength, but without any further presumptions, additional calculations were performed using (19). However, the length of reinforcement was now such that the required strength $k_t/\gamma H$ was not less than that from (24). To achieve the assumed triangular distribution of the limit force, the reinforcement layers of equal strength were distributed with spacing decreasing toward the slope base. Assuming that each reinforcement layer is at the centroid of its respective trapezoidal distribution segment, depth z_i of reinforcement layers was calculated from the following expression:

$$z_i = \frac{2}{3} nH \left[\sqrt{\left(\frac{i}{n}\right)^3} - \sqrt{\left(\frac{i-1}{n}\right)^3} \right], \quad i = 1, 2, \ldots, n \qquad (26)$$

where n = number of layers. The optimization technique was used (θ_0 and θ_h being variable) to find maximum L/H. Some numerical results are shown in columns 6 and 7 in Table 2, and an example is shown in Fig. 9.

The slope in Fig. 9 has an inclination of 80°, internal friction angle of the fill $\varphi = 30°$, and $f_b = 0.5$ ($r_u = 0$). The method used leads to a lower bound on the length of reinforcement, and, therefore, the maximum of the required length was sought [calculated length is not a strict bound in the theoretical sense because of the approximation in (13)]. The solution converged to the maximum of $L/H = 0.570$ (±0.005) for some range of initial parameters used in the optimization procedure. The failure surface associated with this solution is shown in Fig. 9(a). This length coincides with that in Jewell's (1990) charts (column 8, Table 2). However, function $L/H(\theta_0, \theta_h)$ for a small number of reinforcement layers is not a single-extremum function, and $L/H = 0.570$ appears to be a local maximum. A better solution can be found where $L/H = 0.645$ (±0.005) with the failure surface illustrated in Fig. 9(b).

The critical length is sensitive to both the number of layers and their distribution. By increasing significantly the number of layers (for instance, to $n = 50$), implicit function $L/H(\theta_0, \theta_h)$ in (19) seems to be less "bumpy" in space θ_0, θ_h, and a single maximum was found, which matches that in columns 8 and 9 (Table 2) surprisingly well ($L/H = 0.565$).

When the reinforcement spacing is small (large number of layers), there is a likelihood of failure where more than one layer is pulled out with a portion of the fill as one rigid block, significantly reducing the pullout force determined for a single layer in (13). Such mechanisms were not investigated here.

The calculations indicate that assumptions in deriving reinforcement length need to be made with caution. Particularly, representing required reinforcement length as independent of the number of layers may be a significant approximation. Calculations revealed that increasing the number of layers leads to a more "regular" required length function, but the calculated required length for a small number of layers is always larger than that for a large number of layers. This conclusion is true for both uniform and triangular distribution of reinforcement.

The required length in charts by Jewell (1990) seems to have been produced for a large number of reinforcement layers. The required length in these charts falls short of those calculated for a small number of layers (for instance six). A remedy for the deficiency in the length so calculated was introduced through an "empirical" notion of the "bond allowance" (or the "load shedding allowance"), as explained in Jewell (1992). While this concept has not been accepted enthusiastically by designers, the additional reinforcement routinely designed when using charts based on triangular distribution [see, e.g., Fig. 8(b,c)] probably compensates for the length deficiency when using a small number of layers.

Comparison of the required reinforcement length to prevent direct sliding from occurring is shown in Table 3. The discrepancies are not significant.

FINAL REMARKS

The required strength and length of reinforcement for uniformly reinforced slopes were calculated using the kinematic approach of limit analysis. This approach, as applied in this paper, leads to the lower bound for the required reinforcement strength for a given slope, or it can be alternatively formulated to yield the upper bound to the critical height of the slope.

The significant difference from existing solutions is in the assumption that the reinforcement is distributed uniformly throughout the slope height, which is commonly adopted in the design of "low slopes." Limit analysis was also used to document that it produces results identical to those available in the literature for the triangular distribution of reinforcement.

The length of reinforcement against overall failure is derived from the criterion that it be fully utilized (i.e., be no longer than necessary). Two equally critical rotational collapse mechanisms can be found for slopes that satisfy this criterion.

The first one involves rupture of all reinforcing layers (with a possible exception of the very top layer/layers). The second one entails layers that may not even intersect the failure surface, while the combination of reinforcement rupture and pullout occurs for other layers (see failure surfaces A and D in Fig. 2). The reinforcement need not be longer than that which renders the second mechanism as critical as the first one.

A feature of a rotational failure mechanism that was not reported earlier is the likelihood of compression in the upper reinforcement layers. This occurs in the presence of substantial pore-water pressure in steep slopes with uniform distribution of reinforcement. This is particularly important since a geosynthetic reinforcement is likely to kink under compression, and such layers need to be excluded from the calculated reinforcement contribution to the slope strength. Another, perhaps less surprising, feature of rotational failures is that for gentle slopes the middle layers may be pulled out whereas the top ones rupture (contrary to the common presumption that the top layer is pulled out first).

The solution presented here requires a larger amount of reinforcement than that in routinely used design charts. The discrepancy in the required amount (or strength) of reinforcement stems from different distributions of the limit force in reinforcement: uniform versus triangular.

The required length of reinforcement is dependent on the total required limit force (strength), frictional interaction of the reinforcement and the fill, number of layers, and their distribution. Both overall (rotational) and direct sliding (translational) failure mechanisms were considered. The required reinforcement length needed to resist overall failure was found to be consistently higher when it is uniformly distributed (as opposed to triangular distribution).

Calculations with a triangular distribution of reinforcement strength suggest that the routinely used design charts (Jewell 1990) predict the required length well for slopes with a large number of layers. The required length is larger, however, if a smaller number of layers is used (for instance six). Because of the increased amount of reinforcement used commonly in design [see Fig. 8(b,c)], there is no concern about insufficient pullout forces when using the existing design charts.

The technique used does not allow one to evaluate the influence of the soil and reinforcement stiffness on the estimates of the required strength of reinforcement. This is a common drawback of any technique based on limit analysis or limit equilibrium. Also, both limit analysis and limit equilibrium methods, when consistently carried out, provide a lower bound to the required strength of reinforcement (k_r or K_{req}). Hence, by definition, they are not conservative. The rotational failure mechanism used in the analysis, however, is known to be the most adverse failure mode, and the results are probably as good as they can be within the framework of limit analysis (or limit equilibrium).

ACKNOWLEDGMENT

Results presented in this paper are based on research supported by the National Science Foundation under grant No. CMS-9634193. This support is greatly appreciated.

APPENDIX I. EXPRESSIONS FOR FUNCTIONS f_1–f_6

Functions f_1–f_3 were given first by Chen et al. (1969) in the context of slope stability analysis, and they are given here for the case of a horizontal crest of the slope (as in Fig. 1)

$$f_1 = \frac{1}{3(1 + 9\tan^2\varphi)}\left[(3\tan\varphi\cos\theta_h + \sin\theta_h)e^{3(\theta_h-\theta_0)\tan\varphi} - 3\tan\varphi\cos\theta_0 - \sin\theta_0\right] \quad (27)$$

$$f_2 = \frac{1}{6}\frac{B}{r_0}\left(2\cos\theta_0 - \frac{B}{r_0}\right)\sin\theta_0 \quad (28)$$

$$f_3 = \frac{1}{6}\frac{H}{r_0}\frac{\sin(\beta + \theta_h)}{\sin\beta}\left(2\cos\theta_h e^{(\theta_h-\theta_0)\tan\varphi} + \frac{H}{r_0}\cot\beta\right)e^{(\theta_h-\theta_0)\tan\varphi} \quad (29)$$

where

$$\frac{B}{r_0} = \frac{1}{\sin\theta_h}\left[\sin(\theta_h - \theta_0) - \frac{H}{r_0}\frac{\sin(\beta + \theta_h)}{\sin\beta}\right] \quad (30)$$

and the ratio H/r_0 is given in (11). Coefficient f_5 is more complex in derivation (Michalowski 1995), and can be calculated from

$$f_5 = \tan\varphi\left[\int_{\theta_0}^{\theta_1}\frac{z_1}{r_0}e^{2(\theta-\theta_0)\tan\varphi}\,d\theta + \int_{\theta_1}^{\theta_h}\frac{z_2}{r_0}e^{2(\theta-\theta_0)\tan\varphi}\,d\theta\right] \quad (31)$$

where z_1/r_0 and z_2/r_0 are given in

$$\frac{z_1}{r_0} = \frac{r}{r_0}\sin\theta - \sin\theta_0 \quad (32a)$$

$$\frac{z_2}{r_0} = \frac{r}{r_0}\sin\theta - \sin\theta_h e^{(\theta_h-\theta_0)\tan\varphi} + \left[\frac{r}{r_0}\cos\theta - \cos\theta_h e^{(\theta_h-\theta_0)\tan\varphi}\right]\tan\beta \quad (32b)$$

with r given in (3). Angle θ_1 needs to be calculated from

$$\cos\theta_1 e^{(\theta_1-\theta_0)\tan\varphi} = \cos\theta_0 - \frac{B}{r_0}\cos\alpha \quad (33)$$

Closed-form solutions to integrals in (31) were found; angle θ_1, however, was calculated numerically from (33). For vertical slopes $\theta_1 = \theta_h$, and the second integral in (31) is equal to zero.

APPENDIX II. REFERENCES

Bishop, A. W., and Morgenstern, N. R. (1960). "Stability coefficients for earth slopes." *Géotechnique*, London, England, 10(4), 129–150.
Chen, W. F. (1975). *Limit analysis and soil plasticity*. Elsevier Science Publisher BV (North-Holland), Amsterdam, The Netherlands.
Chen, W. F., Giger, M. W., and Fang, H. Y. (1969). "On the limit analysis of stability of slopes." *Soils and Found.*, 9(4), 23–32.
de Buhan, P., Mangiavacchi, R., Nova, R., Pellegrini, G., and Salençon, J. (1989). "Yield design of reinforced earth walls by homogenization method." *Géotechnique*, London, England, 39(2), 189–201.
Drucker, D. C., Prager, W., and Greenberg, H. J. (1952). "Extended limit design theorems for continuous media." *Quarterly Appl. Math.*, 9(4), 381–389.
Jewell, R. A. (1990). "Revised design charts for steep reinforced slopes." *Reinforced embankments, theory and practice*, Thomas Telford, London, England, 1–30.
Jewell, R. A. (1992). "Strength and deformation in reinforced soil design." *Proc., 4th Int. Conf. on Geotextiles, Geomembranes and Related Products*, A. A. Balkema, Rotterdam, The Netherlands, 913–946.
Leshchinsky, D., and Boedecker, R. H. (1989). "Geosynthetic reinforced soil structures." *J. Geotech. Engrg.*, ASCE, 115(10), 1459–1478.
Michalowski, R. L. (1995). "Slope stability analysis: a kinematical approach." *Geotechnique*, London, England, 45(2), 283–293.
Michalowski, R. L. (1996). "Instability patterns of reinforced-soil structures." *Proc., Int. Symp. on Earth Reinforcement, Vol. 1*, H. Ochiai, N. Yasufuku, and K. Omine, eds., A. A. Balkema, Rotterdam, The Netherlands, 809–813.
Michalowski, R. L., and Zhao, A. (1994). "Effect of reinforcement length and distribution on safety of slopes." *Proc., 5th Int. Conf. on Geotextiles, Geomembranes and Related Products, Vol. 1*, Int. Geotextile Soc., Singapore, 495–498.
Michalowski, R. L., and Zhao, A. (1995). "Continuum versus structural approach to stability of reinforced soil." *J. Geotech. Engrg.*, ASCE, 121(2), 152–162.
Sawicki, A., and Leśniewska, D. (1989). "Limit analysis of cohesive

slopes reinforced with geotextiles." *Comp. and Geotech.*, 7(1 and 2), 53–66.
Schmertmann, G. R., Chouery-Curtis, V. E., Johnson, R. D., and Bonaparte, R. (1987). "Design charts for geogrid-reinforced soil slopes." *Proc., Geosynthetics '87, Vol. 1*, Industrial Fabrics Assn. Int., St. Paul, Minn., 108–120.
Wright, S. G., and Duncan, J. M. (1991). "Limit equilibrium stability analyses for reinforced slopes." *Transp. Res. Rec. 1330*, Transp. Res. Board, Washington, D.C., 40–46.

APPENDIX III. NOTATION

The following symbols are used in this paper:

$\dot{D}$ = energy dissipation rate;
F = factor of safety;
f_b = bond coefficient ($\mu_b = f_b \tan \varphi$);
f_d = direct sliding coefficient ($\mu_d = \tan \varphi_w = f_d \tan \varphi$);
H = slope height;
k_t = tensile strength of reinforcement per unit area of reinforced soil mass;
$k_t/\gamma H$ = dimensionless required reinforcement strength;
L = reinforcement length;
$(L/H)_{ds}$ = dimensionless required reinforcement length against direct sliding;
$(L/H)_{ovrl}$ = dimensionless required reinforcement length against overall failure;
l_e = effective length of reinforcement;
n = number of reinforcement layers;
$\mathbf{n}$ = unit vector in direction of reinforcement;
r = log-spiral radius;
r_u = pore pressure coefficient ($u = r_u \gamma z$);
T_p = pullout force for single reinforcement layer per unit width;
T_t = tensile strength of single reinforcement layer per unit width;
u = pore-water pressure;
$\mathbf{v}_i$ = velocity vector;
$\dot{W}$ = rate of work of external forces;
z_i = depth of reinforcement layer i below crest;
z_i^* = overburden depth of reinforcement layer i;
β = slope inclination angle;
γ = unit weight of soil;
θ = polar coordinate (angle);
θ_0, θ_n = magnitudes of θ used to describe failure surface;
φ = internal friction angle of fill;
φ_d = internal friction angle needed to maintain limit equilibrium [$\tan \varphi_d = (\tan \varphi)/F$];
φ_w = geosynthetic-fill friction angle in direct sliding; and
$\dot{\omega}$ = rotational velocity.